

Conference materials

UDC 524.354.6

DOI: <https://doi.org/10.18721/JPM.161.256>

## Middle-aged gamma-ray pulsar J0554+3107 in X-rays

A.S. Tanashkin<sup>✉</sup>, A.V. Karpova, Yu.A. Shibano, A.Yu. Potekhin, D.A. Zyuzin

Ioffe Institute, St. Petersburg, Russia

<sup>✉</sup>artyom.tanashkin@gmail.com

**Abstract.** We present some results of X-ray observations of the middle-aged  $\gamma$ -ray pulsar J0554+3107 with *XMM-Newton*. For the first time, we detected X-ray pulsations with the J0554+3107 spin period from the presumed X-ray counterpart, thus confirming its pulsar nature. The pulsed fraction in the 0.2–2 keV band is  $25\pm 6\%$ . The pulsar spectrum can be fitted by the model consisting of thermal and non-thermal components. To describe the former, we created and applied hydrogen atmosphere models for neutron stars with dipole magnetic fields. In addition, an absorption feature at 0.34 keV is required to fit the spectrum. The spectral analysis implies that J0554+3107 has the effective temperature of  $\sim 47\pm 2$  eV. The analysis also indicates that J0554+3107 may be a rather heavy neutron star with the mass of  $\sim 1.9\pm 0.2 M_{\odot}$ . Implementing the relation between the interstellar absorption and the distance in the pulsar direction, we obtained the distance to the pulsar to be about 2 kpc. Implications of the results for cooling scenarios of neutron stars and the equation of state of supra-dense matter in their cores are briefly discussed.

**Keywords:** neutron stars, pulsars, neutron star cooling, supra-dense matter

**Citation:** Tanashkin A.S., Karpova A.V., Shibano Yu.A., Potekhin A.Yu., Zyuzin D.A., Middle-aged gamma-ray pulsar J0554+3107 in X-rays, St. Petersburg State Polytechnical University Journal. Physics and Mathematics. 16 (1.2) (2023) 370–376. DOI: <https://doi.org/10.18721/JPM.161.256>

This is an open access article under the CC BY-NC 4.0 license (<https://creativecommons.org/licenses/by-nc/4.0/>)

Материалы конференции

УДК 524.354.6

DOI: <https://doi.org/10.18721/JPM.161.256>

## Рентгеновские наблюдения гамма-пульсара J0554+3107

А.С. Танашкин<sup>✉</sup>, А.В. Карпова, Ю.А. Шибанов, А.Ю. Потехин, Д.А. Зюзин

Физико-технический институт им. А.Ф. Иоффе РАН, Санкт-Петербург, Россия

<sup>✉</sup>artyom.tanashkin@gmail.com

**Аннотация.** В работе представлены результаты рентгеновских наблюдений гамма-пульсара среднего возраста J3107+0554, выполненных при помощи обсерватории *XMM-Newton*. Нами впервые обнаружены пульсации излучения с периодом J0554+3107 от предполагаемого рентгеновского двойника, что подтверждает его пульсарную природу. Доля пульсирующей составляющей в диапазоне 0,2–2 кэВ равна  $25\pm 6\%$ . Спектр пульсара хорошо аппроксимируется моделью, включающей в себя тепловую и нетепловую компоненты. Для описания первой нами были рассчитаны сетки моделей водородных атмосфер нейтронных звезд с сильными магнитными полями. Кроме того, для корректного описания наблюдаемого спектра требуется включение в модель линии поглощения на энергии 0,34 кэВ. По результатам спектрального анализа эффективная температура J0554+3107 составляет  $\sim 47\pm 2$  эВ. Из него также следует, что масса нейтронной звезды равна  $\sim 1,9\pm 0,2 M_{\odot}$ . Используя соотношение между межзвездным поглощением и расстоянием в направлении на пульсар, мы получили оценку на расстояние до него около 2 кпк. В свете полученных результатов кратко обсуждается проблема остывания нейтронных звезд и уравнений состояния сверхплотного вещества в их ядрах.



**Ключевые слова:** нейтронные звезды, пульсары, остывание нейтронных звезд, сверхплотное вещество

Ссылка при цитировании: Танашкин А.С. и др. Рентгеновские наблюдения гамма-пульсара J0554+3107 // Научно-технические ведомости СПбГПУ. Физико-математические науки. 2023. Т. 16. № 1.2. С. 370–376. DOI: <https://doi.org/10.18721/JPM.161.256>

Статья открытого доступа, распространяемая по лицензии CC BY-NC 4.0 (<https://creativecommons.org/licenses/by-nc/4.0/>)

## Introduction

The middle-aged pulsar J0554+3107 (hereafter J0554) discovered in  $\gamma$ -rays with the *Fermi* observatory has the spin period  $P = 465$  ms, the characteristic age  $t_c = 52$  kyr, the spin-down luminosity  $\dot{E} = 5.6 \cdot 10^{34}$  erg  $s^{-1}$  and the characteristic magnetic field  $\dot{B}_c = 8.2 \cdot 10^{12}$  G [1]. In the radio, only upper limits on the pulsar flux density were set [1–3]. J0554 is likely associated with the shell-type supernova remnant (SNR) G179.0+2.6 [1]. The distance to the latter is not well constrained: different relations between the radio surface brightness and the SNR diameter (so-called  $\Sigma$ – $d$  relations) result in about 3–6 kpc [4–6]. On the other hand, studies of the interstellar extinction along the line of sight to the remnant suggest a smaller distance of  $\sim 0.9$  kpc, according to the model of Zhao et al. [7]. These estimates roughly agree with the ‘pseudo-distance’ to J0554 of 1.9 kpc, which is derived from the empirical correlation between the distance and the pulsar  $\gamma$ -ray flux [8] and is uncertain within a factor of 2–3. The likely pulsar X-ray counterpart was found in the *Swift* data [9]. This is a soft source whose spectrum can be described by the black body or hydrogen neutron star (NS) atmosphere models with effective temperatures of  $\sim 50$ – $100$  eV. Since only 17 counts were detected, an accurate spectral analysis is impossible. Detection of pulsations with the J0554 spin period from the presumed X-ray counterpart would directly confirm its pulsar nature. Here we briefly report some results of our deeper X-ray observations of J0554 with *XMM-Newton*.

## *XMM-Newton* data and imaging

The observations were performed on 2021 October 7 (ObsID 0883760101, PI A. Karpova) with a total exposure of about 45 ks. Two MOS detectors were operated in the Full Frame mode while the Large Window mode was chosen for the pn camera. The data were reprocessed using the *XMM-Newton* Science Analysis Software v.19.1.0 package. We filtered out the periods of flaring background activity that resulted in exposures of 44.3, 44.5 and 38.8 ks for MOS1, MOS2 and pn detectors. The exposure-corrected combined (MOS+pn) image of the J0554 field, constructed utilizing the ‘images’ script [10], is shown in Fig. 1. A bright X-ray point-like source is clearly seen at the  $\gamma$ -ray position of J0554 [1], thus confirming the *Swift* X-ray counterpart at much higher significance. We derived its coordinates R.A. =  $05^{\text{h}}54^{\text{m}}05.^{\text{s}}067(10)$  and Dec. =  $+31^{\circ}07'41.''40(13)$  with the `EDETECT_CHAIN` tool (errors in parentheses are  $1\sigma$  pure statistical uncertainties). We found no evidence of extended emission (e.g. the pulsar wind nebula) around J0554. Due to the wide wings of the *XMM-Newton* point spread function (PSF) it can be blurred with the pulsar. However, the brightness radial profile of the source is in agreement with the PSF shape and, therefore, no extended emission is resolved.

## Timing

To search for pulsations with the pulsar spin period, we used the pn data whose time resolution was  $\sim 48$  ms. We extracted events in the 0.2–2 keV band from the  $22''$ -radius circle and applied the barycentric correction using the DE405 ephemeris. The selected aperture contains 1026 source counts. We then ran  $Z_n^2$ -test [11] in the 2.1501–2.1509 Hz range, where the number of harmonics  $n$  was varied from 1 to 5. It revealed pulsations at the frequency of 2.150474376(14) Hz. The contribution from harmonics higher than 2 is not statistically significant. The maximum  $Z_2^2$  of 42.7 corresponds to the detection confidence level of  $\sim 4.7 \sigma$ .

The obtained frequency is slightly higher than the value of 2.150474376(14) Hz predicted from the *Fermi* timing solution [1] at the epoch of the *XMM-Newton* observations. About 8 years passed between the  $\gamma$ -ray and X-ray observations so the discrepancy could arise from the pulsar timing noise or glitches. The detected pulsations firmly establish the pulsar nature of the X-ray source.

The J0554 folded light curve in the 0.2–2 keV band is shown in Fig. 2. We calculated the pulsed fraction (PF) using the method from [12]. The resulting background corrected value is  $25 \pm 6\%$ . Above 2 keV there are only  $\lesssim 2\%$  of the total number of source counts, which precludes any definite conclusions about pulsations in the hard band.

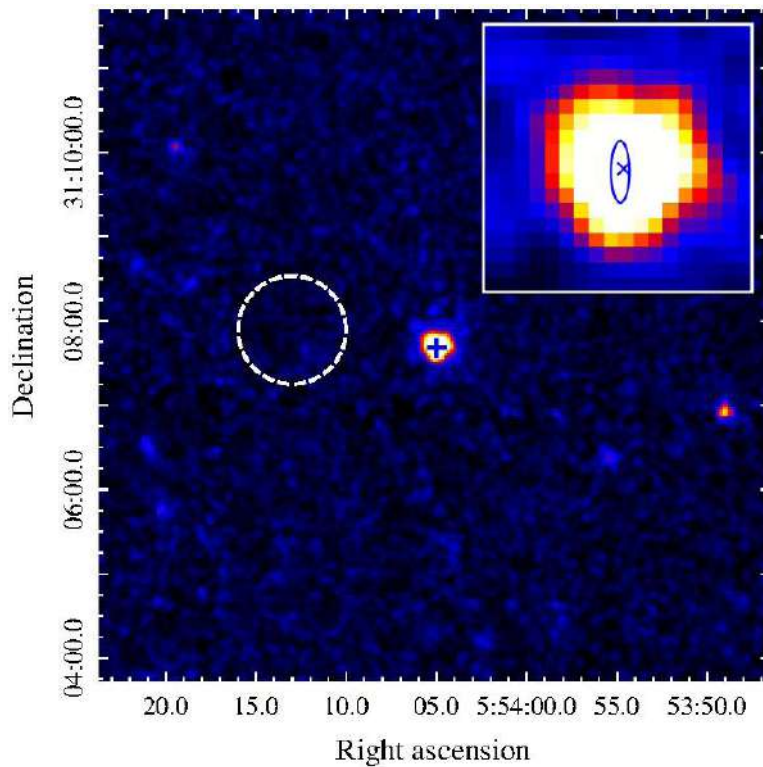


Fig. 1.  $8' \times 8'$  *XMM-Newton* exposure-corrected combined image of the J0554 field in the 0.2–2 keV band.

The pulsar  $\gamma$ -ray position [1] is marked by the cross. The dashed circle encloses the region used for the background. The inset shows the zoomed-in  $0.6' \times 0.6'$  region around the J0554 X-ray counterpart, whose position is shown by the 'X' symbol. The ellipse shows  $1\sigma$  position uncertainties of the pulsar in  $\gamma$ -rays, which is a combination of the *Fermi* position uncertainties and the *XMM-Newton* absolute pointing accuracy of  $1.''2$  (see <https://xmmweb.esac.esa.int/docs/documents/CAL-TN-0018.pdf>)

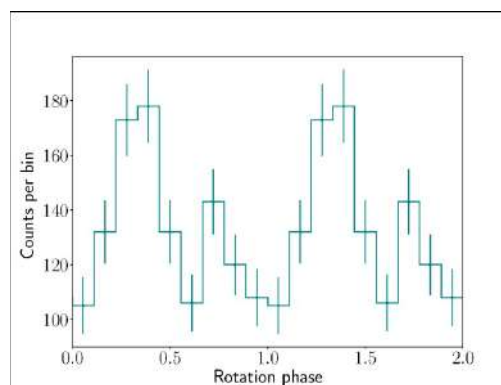


Fig. 2. J0554 pulse profile in the 0.2–2 keV band



### Spectral analysis

We extracted the J0554 spectra from the MOS and pn data using 19''-radius aperture. For the background, we used the circle region shown in Fig. 1. We fitted the spectra simultaneously in the 0.2–10 keV band utilizing the X-Ray Spectral Fitting Package (XSPEC) v.12.11.1 [13]. To account for the interstellar medium (ISM) absorption, we applied the TBABS model with the WILM abundances [14].

As a preliminary step, all spectra were grouped to ensure at least 25 counts per energy bin to use the  $\chi^2$ -statistics. At first, we tried the POWERLAW (PL) model which can represent the non-thermal emission of the NS magnetosphere origin. Though it resulted in a statistically acceptable fit, it requires the photon index  $\Gamma \approx 7$ , while the typical values for pulsars are  $\lesssim 3$  [15]. Such an unrealistically high  $\Gamma$  may indicate the presence of a thermal component. To fit the latter, we created an NS hydrogen atmosphere model NSMDINTB, which was computed using an advanced version of the code described in [16]. This model takes into account the effects of incomplete ionization of plasma, atomic center-of-mass motion across the magnetic field and polarization of vacuum (see, e.g., [17] for review and references). The phase-averaged spectra of radiation from the entire surface, as seen by a distant observer, were computed assuming a dipole magnetic field and taking into account the effects of General Relativity, using the same approach as described in Appendix A of [18]. The magnetic field at the pole  $B_p$  was set to  $10^{13}$  G, which is close to the J0554 spin-down field. The following model parameters are variable: the NS mass  $M$  and the radius  $R$ , the angle  $\alpha$  between the rotation and the magnetic axes, the angle  $\zeta$  between the rotation axis and the line of sight, the distance  $D$ , and the redshifted effective temperature  $T^\infty = T / (1+z_g)$ , where  $z_g$  is the gravitational redshift. This model describes the spectra poorly with  $\chi^2/\text{d.o.f.} = 62/39$  (d.o.f.  $\equiv$  degrees of freedom). The fit becomes statistically acceptable ( $\chi^2/\text{d.o.f.} = 41/36$ ) if we add the absorption Gaussian line at  $\sim 0.35$  keV. For the latter, we used the model GABS. However, the residuals show slight flux excess over the model in the hard band ( $\gtrsim 2$  keV). Thus, we included the PL component in the model and obtained  $\chi^2/\text{d.o.f.} = 39/34$ .

Table 1

**Best-fitting parameters for the (NSMDINTB+PL) $\times$ GABS model**

$N_{\text{H}}, 10^{21} \text{ cm}^{-2}$	$D, \text{ kpc}$	$M, M_{\odot}$	$R, \text{ km}$	$T^\infty, \text{ eV}$	$\Gamma$	$\log L_{\text{X}}, \text{ erg s}^{-1}$	$E_0, \text{ eV}$	EW, eV
$1.62^{+0.08}_{-0.06}$	$2.0^{+0.2}_{-0.4}$	$1.9^{+0.2}_{-0.2}$	$13.5^{+1.2}_{-1.7}$	$47^{+2}_{-2}$	$2.2^{+0.6}_{-0.4}$	$30.21^{+0.15}_{-0.30}$	$340^{+40}_{-40}$	$150^{+120}_{-40}$

Notes: Errors correspond to 68 % credible intervals.  $L_{\text{X}}$  is the non-thermal luminosity in the 2–10 keV band,  $E_0$  and EW are the center and equivalent width of the Gaussian absorption line. Angles  $\alpha$  and  $\zeta$  are poorly constrained and thus not presented.  $W/\text{d.o.f.} = 228/211$  and  $\chi^2/\text{d.o.f.} = 43/34$ .

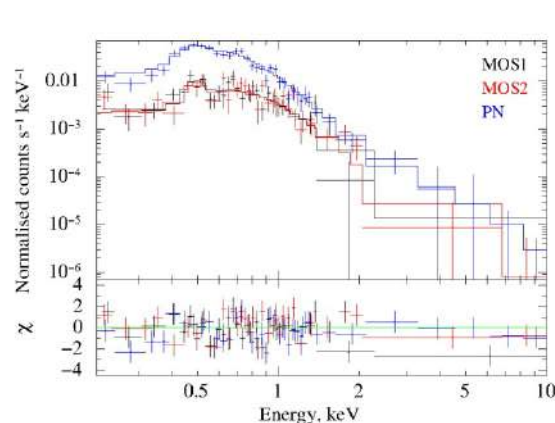


Fig. 3. J0554 spectra, best-fitting model and residuals

Since the number of counts from the pulsar is not large, to robustly constrain model parameters we rebinned the spectra to have at least 1 count per energy bin and applied the  $W$ -statistics [19], which is suitable for the Poisson data. We then performed the Bayesian parameter estimation using the python package `EMCEE` [20], an implementation of affine-invariant ensemble sampler for Markov chain Monte Carlo (MCMC) [21]. Such a method makes it possible to include some prior information in the fitting procedure. We used the 3D extinction map [22] to estimate the distance to the pulsar. The selective reddening  $E(B - V)$  was transformed to the equivalent hydrogen column density  $N_{\text{H}}$ , which is responsible for the ISM absorption in X-rays, using the relation from [23]. Finally, we constrained the photon index  $\Gamma$  between 0.5 and 3, as appropriate for pulsars [15].

The best-fitting parameters, corresponding to the maximum values of probability density, are presented in Table 1 while the J0554 spectrum with the best-fitting model is shown in Fig. 3. We checked the fit quality by calculating the  $\chi^2$ -statistics value for the spectra grouped to ensure at least 25 counts per bin. Inclusion of the priors in the fitting procedure led to some deviation of this value from the preliminary one.

### Discussion and conclusions

Using *XMM-Newton* we have confirmed the *Swift* X-ray counterpart candidate of J0554 and surely established its pulsar nature by revealing the X-ray pulsations with the pulsar spin period. We found that the J0554 time-integrated spectrum in the 0.2–10 keV band is well fitted by the model containing the thermal and non-thermal components and the absorption line. The thermal component can be produced by the hydrogen magnetized atmosphere of an NS with the mass of  $1.9 \pm 0.2 M_{\odot}$  and the redshifted effective temperature of  $47 \pm 2$  eV. Using the extinction–distance relation, we estimated the distance to J0554 to be in the range of 1.6–2.2 kpc, which is compatible with the ‘pseudo-distance’ of 1.9 kpc. The pulsar non-thermal X-ray luminosity in the 2–10 keV range  $L_x = (1.6 \pm 0.7) \cdot 10^{30}$  erg s<sup>-1</sup>. The corresponding efficiency of generation of X-ray photons from the pulsar rotation energy losses is  $\eta_x = L_x / \dot{E} \sim 10^{-5}$ , where  $\dot{E} = 1.4 \cdot 10^{35}$  erg s<sup>-1</sup> is calculated for the best-fitting NS mass and radius. These values are in agreement with the empirical relations  $L_x(t_c)$  and  $\eta_x(t_c)$  obtained for other pulsars [24].

As for the absorption feature at 0.34 keV, its origin is unclear. If it is produced near the NS surface, its unredshifted energy should be  $\sim 0.4 - 0.5$  keV. If this is a cyclotron absorption line produced by electrons, the corresponding magnetic field is  $\sim 4 \cdot 10^{10}$  G, which is much lower than the characteristic field  $B_c = 8.2 \cdot 10^{12}$  G. This implies that such a line should be created in NS radiation belts [25]. On the other hand, if it is the proton cyclotron line, the magnetic field is  $\gtrsim 7 \cdot 10^{13}$  G, an order of magnitude higher than  $B_c$  and the  $B$  values used in our atmosphere modeling. Such a proton cyclotron line might indicate the presence of strong non-dipolar field components (cf. [26, 27]; also see [28] and references therein). The absorption feature can be also produced by atomic transitions in the NS atmosphere composed of heavier chemical elements (e.g., see Fig. 16 in [29] for neon). One explanation that is more possible is an instrumental artifact. The feature is not prominent in the MOS spectra likely due to the much lower count statistics. We could check the presence of the line in pn spectra of other sources in the J0554 field, but, unfortunately, they are not bright enough for such analysis.

The best-fitting atmosphere model provides the PF in the 0.2–2 keV band up to  $\sim 20\%$ , which is compatible with the observed value of  $25 \pm 6\%$ . Because of the low count statistics, we cannot make definite conclusions about pulsations in the hard band where the PL component dominates in the pulsar spectrum. Though the PL contribution to the pulsar flux in the 0.2–2 keV band is less than that of the thermal component, the former can increase the model predicted PF and lead to apparent asymmetry of the observed pulse profile.

The derived bolometric thermal luminosity of J0554  $L_{\text{bol}} \approx 1.8 \cdot 10^{32}$  erg s<sup>-1</sup> appears to be significantly lower than the values predicted for a 52 kyr old NS by the so-called ‘minimal cooling’ scenario [30,31], which assumes that the heat losses mainly occur via neutrino generated by modified Urca processes in the NS core. On the other hand, it is much higher than the values predicted for this age by the enhanced cooling scenario, which involves direct Urca processes operating when the NS mass  $M$  exceeds some threshold value  $M_{\text{DU}}$  (see, e.g., [17] for review and references). The derived  $L_{\text{bol}}$  can be brought to an agreement with the enhanced cooling scenario, if the true age of J0554 is much smaller than  $t_c$ , which is not unusual for the pulsars (see [32]). An alternative is that  $M$  only slightly exceeds the threshold, so that the direct Urca processes are working only in a small central part of the NS core. Another possibility is that  $M$  is only slightly smaller than  $M_{\text{DU}}$ . In this case, the modified



Urca processes are strongly enhanced, so that the NS cools faster, as recently shown by Shternin et al. [33]. The value of  $M_{\text{DU}}$  is currently uncertain: it depends on the composition and equation of state of the NS matter and strongly varies from one theoretical model to another. For example, the modern model BSk24 predicts  $M_{\text{DU}} \approx 1.6 M_{\odot}$  [34], while another widely used model APR gives  $M_{\text{DU}} \approx 2.0 M_{\odot}$  [35]. Both values lie within the  $2\sigma$  uncertainty interval of the  $M$  value given in Table 1.

Deeper X-ray observations are required to better constrain the shape of the pulse profile, to perform the phase-resolved spectral analysis and thereby to establish the nature of the low energy spectral feature and the pulsar geometry.

### Acknowledgements

We are grateful to V.F. Suleimanov for providing calculations of specific spectral fluxes from hydrogen atmospheres of NSs with strong magnetic fields. DAZ thanks Pirinem School of Theoretical Physics for hospitality.

### REFERENCES

1. **Pletsch H. J., et al.**, Einstein@Home Discovery of Four Young Gamma-Ray Pulsars in Fermi LAT Data, *Astrophys. J.* 779 L11 (2013).
2. **Tyul'bashev S.A., Kitaeva M.A., Tyulbasheva G.E.**, Search for Periodic Emission from Five Gamma-Ray Pulsars at the Frequency of 111 MHz, *Astronomy Reports* 65 (2021) 819–25.
3. **Griesmeier J.M., Smith D.A., Theureau G., Johnson T.J., Kerr M., Bondonneau L., Cognard I., Serylak M.**, Follow-up of 27 radio-quiet gamma-ray pulsars at 110–190 MHz using the international LOFAR station FR606, *Astron. Astrophys.* 654 A43 (2021).
4. **Case G.L., Bhattacharya D.**, A New  $\sigma$ -D Relation and Its Application to the Galactic Supernova Remnant Distribution, *Astrophys. J.* 504 (1998) 761–72.
5. **Guseinov O.H., Ankay A., Sezer A., Tagieva S.O.**, The relation between the surface brightness and the diameter for galactic supernova remnants, *Astronomical and Astrophysical Transactions* 22 273 (2003).
6. **Pavlovic M.Z., Dobardzic A., Vukotic B., Urosevic D.**, Updated Radio Sigma-D Relation for Galactic Supernova Remnants, *Serbian Astronomical Journal* 189 (2014) 25–40.
7. **Zhao H., Jiang B., Li J., Chen B., Yu B., Wang Y.**, A Systematic Study of the Dust of Galactic Supernova Remnants. I. The Distance and the Extinction, *Astrophys. J.* 891 137 (2020).
8. **Saz Parkinson P. M. et al.**, Eight  $\gamma$ -ray Pulsars Discovered in Blind Frequency Searches of Fermi LAT Data, *Astrophys. J.* 725 (2010) 571–84.
9. **Zyuzin D.A., Karpova A.V., Shibanov Y.A.**, X-ray counterpart candidates for six new  $\gamma$ -ray pulsars, *Mon. Not. R. Astron. Soc.* 476 (2018) 2177–85.
10. **Willatt R., Ehle M.**, Guide for use of the images script. URL: <https://www.cosmos.esa.int/documents/332006/641121/README.pdf>. Accessed Oct. 9, 2022.
11. **Buccheri R., et al.**, Search for pulsed gamma-ray emission from radio pulsars in the COS-B data, *Astron. Astrophys.* 128 (1983) 245–51.
12. **Swanepoel J.W.H., de Beer C.F., Loots H.**, Estimation of the Strength of a Periodic Signal from Photon Arrival Times, *Astrophys. J.* 467 261 (1996).
13. **Arnaud K.A.**, Astronomical Data Analysis Software and Systems V, In: *Astronomical Society of the Pacific Conference Series* vol. 101 ed. Jacoby G. H. and Barnes J. (1996) 17.
14. **Wilms J., Allen A., McCray R.**, On the Absorption of X-Rays in the Interstellar Medium, *Astrophys. J.* 542 (2000) 914–24.
15. **Kargaltsev O., Pavlov G.G.**, 40 Years of Pulsars: Millisecond Pulsars, Magnetars and More, In: *American Institute of Physics Conference Series* vol. 983 ed. Bassa C., Wang Z., Cumming A. and Kaspi V.M. (2008) 171–85.
16. **Suleimanov V., Potekhin A.Y. and Werner K.**, Models of magnetized neutron star atmospheres: thin atmospheres and partially ionized hydrogen atmospheres with vacuum polarization, *Astron. Astrophys.* 500 (2009) 891–9.
17. **Potekhin A.Y., De Luca A., Pons J.A.**, Neutron Stars Thermal Emitters, *Space Sci. Rev.* 191 (2015) 171–206.
18. **Zyuzin D.A., Karpova A.V., Shibanov Y.A., Potekhin A.Y., Suleimanov V.F.**, Middle aged  $\gamma$ -ray pulsar J1957+5033 in X-rays: pulsations, thermal emission, and nebula, *Mon. Not. R. Astron. Soc.* 501 (2021) 4998–5011.

19. **Wachter K., Leach R., Kellogg E.**, Parameter estimation in X-ray astronomy using maximum likelihood, *Astrophys. J.* 230 (1979) 274–87.
20. **Foreman-Mackey D., Hogg D.W., Lang D., Goodman J.**, emcee: The MCMC Hammer, *Publ. Astron. Soc. Pacific* 125 306 (2013).
21. **Goodman J., Weare J.**, Ensemble samplers with affine invariance, *Communications in Applied Mathematics and Computational Science* 5 (2010) 65–80.
22. **Green G.M., Schlafly E., Zucker C., Speagle J.S., Finkbeiner D.**, A 3D Dust Map Based on Gaia, Pan-STARRS 1, and 2MASS, *Astrophys. J.* 887 93 (2019).
23. **Foight D.R., Güver T., Uzel F. and Slane P.O.**, Probing X-Ray Absorption and Optical Extinction in the Interstellar Medium Using Chandra Observations of Supernova Remnants, *Astrophys. J.* 826 66 (2016).
24. **Zharikov S., Mignani R.P.**, On the PSR B1133+16 optical counterpart, *Mon. Not. R. Astron. Soc.* 435 (2013) 2227–33.
25. **Luo Q., Melrose D.**, Pulsar radiation belts and transient radio emission, *Mon. Not. R. Astron. Soc.* 378 (2007) 1481–90.
26. **Bilous A.V., et al.**, A NICER View of PSR J0030+0451: Evidence for a Global-scale Multipolar Magnetic Field, *Astrophys. J.* 887 L23 (2019).
27. **Lockhart W., Gralla S. E., Uzel F., Psaltis D.**, X-ray light curves from realistic polar cap models: inclined pulsar magnetospheres and multipole fields, *Mon. Not. R. Astron. Soc.* 490 (2019) 1774–83.
28. **Mereghetti S., Pons J.A., Melatos A.**, Magnetars: Properties, Origin and Evolution, *Space Sci. Rev.* 191 (2015) 315–38.
29. **Mori K., Ho W.C.G.**, Modelling mid-Z element atmospheres for strongly magnetized neutron stars, *Mon. Not. R. Astron. Soc.* 377 (2007) 905–19.
30. **Gusakov M.E., Kaminker A.D., Yakovlev D.G., Gnedin O.Y.**, Enhanced cooling of neutron stars via Cooper-pairing neutrino emission, *Astron. Astrophys.* 423 (2004) 1063–71.
31. **Page D., Lattimer J.M., Prakash M., Steiner A.W.**, Minimal Cooling of Neutron Stars: A New Paradigm, *Astrophys. J. Suppl. Ser.* 155 (2004) 623–50.
32. **Potekhin A.Y., Zyuzin D.A., Yakovlev D.G., Beznogov M.V., Shibano Y.A.**, Thermal luminosities of cooling neutron stars, *Mon. Not. R. Astron. Soc.* 496 (2020) 5052–71.
33. **Shternin P.S., Baldo M., Haensel P.**, In-medium enhancement of the modified Urca neutrino reaction rates, *Physics Letters B* 786 (2018) 28–34.
34. **Pearson J.M., Chamel N., Potekhin A.Y., Fantina A.F., Ducoin C., Dutta A.K., Goriely S.**, Unified equations of state for cold non-accreting neutron stars with Brussels-Montreal functionals - I. Role of symmetry energy, *Mon. Not. R. Astron. Soc.* 481 (2018) 2994–3026.
35. **Akmal A., Pandharipande V.R., Ravenhall D.G.**, Equation of state of nucleon matter and neutron star structure, *Phys. Rev. C* 58 (1998) 1804–28.

## THE AUTHORS

**TANASHKIN Artyom S.**  
 artyom.tanashkin@gmail.com  
 ORCID: 0000-0002-3340-0938

**POTEKHIN Alexander Y.**  
 palex@astro.ioffe.ru  
 ORCID: 0000-0001-9955-4684

**KARPOVA Anna V.**  
 karpann@astro.ioffe.ru  
 ORCID: 0000-0002-4211-5856

**ZYUZIN Dmitry A.**  
 da.zyuzin@gmail.com  
 ORCID: 0000-0002-8521-9233

**SHIBANOV Yury A.**  
 shib@astro.ioffe.ru

*Received 27.10.2022. Approved after reviewing 10.11.2022. Accepted 11.11.2022.*